

Water Density in the Electric Double Layer at the Insulator/Electrolyte Solution Interface

Aleksey M. Tikhonov*

University of Chicago, Consortium of Advanced Radiation Sources, and Brookhaven National Laboratory,
National Synchrotron Light Source, Beamline X19C, Upton, New York 11973

Received: September 30, 2005; In Final Form: December 11, 2005

I studied the spatial structure of the thick transition region between *n*-hexane and a colloidal solution of 7-nm silica particles by X-ray reflectivity and grazing incidence small-angle scattering. The interfacial structure is discussed in terms of a semiquantitative interface model wherein the potential gradient at the *n*-hexane/sol interface reflects the difference in the potentials of “image forces” between the cationic Na⁺ and anions (nanoparticles) and the specific adsorption of surface charge at the interface between the adsorbed layer and the solution, as well as at the interface between the adsorbed layer and *n*-hexane. The X-ray scattering data revealed that the average density of water in the field $\sim 10^9$ – 10^{10} V/m of the electrical double layer at the hexane/silica sol interface is the same as, or only few percent higher (1–7%) than, its density under normal conditions.

Introduction

The properties of water in the transition region at a charged interface, where an electrical field, *E*, reaches enormously high values of 10^8 – 10^{11} V/m, is of considerable fundamental interest in electrochemistry and biology. A decade ago, several authors obtained ambiguous results on the arrangement of water molecules in the electric double layer at a metal electrode's surface. Thus, Toney et al.¹ reported an exceptionally high density of water in the first two to three layers adsorbed at the Ag electrode's surface, such that this “surface water” was twice as dense as bulk water under normal conditions. Wang et al.² who systematically studied by X-ray scattering a variety of inorganic electrolyte solutions at the electrolyte/Au electrode interface also observed a high electron density in the electric double layer, but related it to the direct adsorption of ions and clusters of gold atoms at the electrode's surface. They further noted that the main problem in interpreting X-ray data is the lack of accurate knowledge of the in-plane structure (morphology) of the metal electrode's surface, so making the interpretation of X-ray reflectivity at the electrode/electrolyte interface controversial.

Danielovich–Ferchmin and Ferchmin studied the relationship between the density of water and the surface charge density in the electrical double layers.³ According to them, in a very strong electric field $E > 10^8$ V/m, the density of water is significantly higher than it is at normal conditions because of the ordering of dipole moments of H₂O along the field, *E*. Accordingly, their result supported Toney et al.'s¹ interpretation of the X-ray scattering experiment at the electrolyte/Ag electrode interface that was based on very strong assumptions about the interfacial structure, i.e., an electrode's surface is atomically smooth, and electrolyte ions in the Stern layer do not adsorb directly to the electrode's surface.

Recently, we studied the transition region between *n*-hexane (insulator) and a nanocolloidal silica solution (electrolyte solution).⁴ The uniqueness of this interfacial electric double layer is that it is 10 times wider than those detailed by Toney et al.¹ and Wang et al.² The electrical charges are well-separated at the interface by a layer of “surface water” of ~ 60 Å thick, so

that its interfacial field, *E*, is as high as $\sim 10^9$ V/m. A field of such strength is impossible to obtain in an electrolytic capacitor, but is common in the first hydration shell of a small inorganic ion (for instance, Na⁺, Cu²⁺, Al³⁺).³ Here, I report the findings on the water density in the electric double layer, which was explored by combining the techniques of X-ray reflectivity and grazing incidence small-angle scattering.

The *n*-hexane/silica sol system offers several advantages for the X-ray scattering experiments compared with electrolyte/metal electrode interfaces. First, the *n*-hexane/water interface has a well-understood in-plane structure that is described by the theory of capillary waves.^{5,6} Second, this oil–water interface has an enhanced structure factor (X-ray reflectivity normalized to the Fresnel function) due to a relatively small difference in the bulk electron densities of water and *n*-hexane.^{4,7} Third, scattering from the hexane/silica sol interface is defined by the interfacial structure. Scattering from the transition region at the electrolyte/metal is very weak in comparison with Bragg diffraction from the electrode's bulk.² Finally, the electric double layer at the hexane/silica sol interface is very wide because of the extremely strong repulsion of nanoparticles from the oil by the forces of electrical imaging. Also, the negative and positive charges are well-separated at the interface by a thick layer of “surface water”. Consequently, the interfacial structure can be resolved by data with relatively poor spatial resolution compared with those required in the experiments of Toney et al.¹ and Wang et al.² (see ref 8).

Experimental Methods

All the data presented in this paper were obtained at beamline X19C, National Synchrotron Light Source, Brookhaven National Laboratory.^{6,9} I employed a monochromatic focused X-ray beam to explore the planar interface between the nonmiscible *n*-hexane and silica solution. At the chosen X-ray wavelength, $\lambda = 0.825 \pm 0.002$ Å, the absorption length for *n*-hexane is approximately 19 mm, allowing thick samples to be studied. A stainless steel sample cell with a rectangular interfacial area (75 mm along and 150 mm across the beam's direction) was placed inside a two-stage thermostat. The temperature in the second stage of the thermostat was stable to better than $\pm 3 \times 10^{-2}$ K. All X-ray scattering measurements were carried out after the sample was equilibrated at $T = 298$ K for at least 12 h.

* E-mail: tikhonov@bnl.gov.

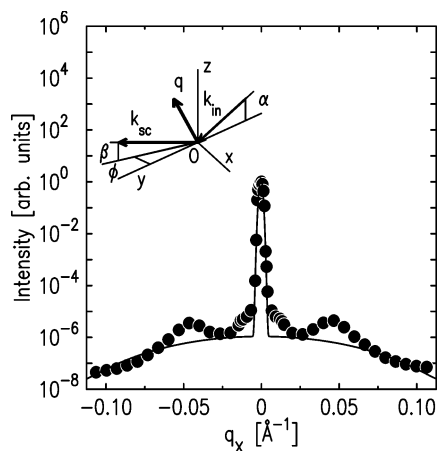


Figure 1. Small-angle scattering from the bulk sample of the silica sol. The central peak at $q_x = 0$ is the transmission beam. The two shoulder peaks at $q_x \approx \pm 0.05 \text{ \AA}^{-1}$ are associated with the principal ring of the small-angle scattering. The solid line is the linear combination of the Gaussian function (the central peak) and the scattering power of a homogeneous sphere 70 \AA in diameter (background). The insert is a sketch of the kinematics of the scattering at the hexane/silica sol interface. The x - y plane coincides with the interface, the axis x is perpendicular to the beam's direction, and the axis z is directed normal to the interface opposite to the gravitational force. \mathbf{k}_{in} and \mathbf{k}_{sc} are, respectively, wave vectors of the incident beam and beam scattered toward the point of observation, and \mathbf{q} is the wave vector transfer, $\mathbf{q} = \mathbf{k}_{in} - \mathbf{k}_{sc}$.

n-Hexane was purchased from Sigma-Aldrich and purified by passing through activated alumina in a chromatography column. Concentrated suspensions of colloidal silica particles in water (obtained from Dupont), of approximately 70 \AA in diameter, D , at $\text{pH} \approx 10$ were stabilized with alkali. The resulting homogeneous solution of NaOH and solid silica particles in water (30% SiO₂ and 0.5% Na by weight) had a specific gravity, ζ , of $1.177 \pm 0.003 \text{ g/cm}^3$. The molar concentration of free hydroxyl ions in the sol bulk is extremely low, $c^- \approx 10^{-4} \text{ mol/L}$, compared with the concentration of sodium ions, $c^+ = f_{\text{Na}\zeta}/M_{\text{Na}} \approx 2.4 \times 10^{-1} \text{ mol/L}$ ($M_{\text{Na}} \approx 23 \text{ g/mol}$ is the atomic weight of Na, and f_{Na} is the weight fraction of sodium in the suspension), because of the adsorption of OH⁻ ions at the silica surface. A particle in the sol can be treated as analogous to a large ion. Therefore, silica sol is a strong electrolyte in which the solutes are completely ionized.

n-Hexane and colloidal silica neither mix on molecular level nor form any silica-stabilized emulsion. The tension, γ , of the hexane/sol interface was approximately 42 mN/m measured by the Wilhelmy plate method. Gravity orients the hexane/silica sol interface so that it is useful to describe the kinematics of scattering in the right-handed rectangular system of the coordinate wherein the origin, O , is situated in the center of the footprint; here, the x - y plane coincides with the interface between the transition region and bulk hexane, the axis x is perpendicular to the beam's direction, and the axis z is directed normal to the interface opposite to the gravitational force (Figure 1). α is the incident angle in the y - z plane, β is the angle in the vertical plane between the direction of scattering and the interface, and ϕ is the angle in the x - y plane between the incident beam's direction and the direction of the scattering. Since the angles were small in my experiments, the components of the wave vector transfer, \mathbf{q} , at small-angle deviations, $\delta\phi$ and $\delta\beta$, from the specular condition, $\alpha = \beta$, and $\phi = 0$, can be written in the following forms:

$$q_x \approx \frac{2\pi}{\lambda} \delta\phi$$

$$q_y \approx \frac{2\pi}{\lambda} \alpha\delta\beta$$

$$q_z \approx \frac{2\pi}{\lambda} (\alpha + \beta) \quad (1)$$

The reflectivity measurements were carried out with the vertical angular acceptance of the detector, $\Delta\beta = 3.4 \times 10^{-2} \text{ deg}$. and its horizontal acceptance at $\Delta\phi = 0.8^\circ$. Measurements of the grazing incidence small-angle scattering were taken with $\Delta\beta = 0.2^\circ$ and $\Delta\phi = 4 \times 10^{-2} \text{ deg}$.

Since $c^- \ll c^+$, a particle in the sol carries a negative charge up to $Z \approx e(c^+N_A/c_b) \approx 700e$ (e is the elementary charge, and N_A is the Avogadro constant). The bulk concentration, c_b , of particles in the suspension was as much as $c_b \approx d_b^{-3} \approx 2 \times 10^{23} \text{ m}^{-3}$. The particle-particle distance, $d_b \approx 170 \text{ \AA}$, was obtained from measuring the small-angle scattering of a bulk sample, which was prepared in 0.5-mm -diameter glass tube. The tube was oriented along the z -axis so that kinematics of the scattering were described by eq 1 at $\alpha = 0$. The value of the scattering vector, $q_0 \approx 0.045 \text{ \AA}^{-1}$, which corresponds to the maxima of the "principal ring" (see Figure 1), defines $d_b \approx 1.23(2\pi/q_0)$ (see, for example, ref 10).

Figure 2a shows X-ray reflectivity normalized to the Fresnel function (structure factor) in the q_z range up to $q_z^{\text{max}} = 0.475 \text{ \AA}^{-1}$, that provides the spatial resolution of the electron density profile across the interface $2\pi/q_z^{\text{max}} \approx 15 \text{ \AA}$. At small q_z , the reflectivity is strongly related to the entire structure of the transition layer. At $q_z > 0.25 \text{ \AA}^{-1}$, the reflection from the surface between layer 1 and the oil is dominant, because this interface has the smallest roughness, σ_0 , defined by the spectrum of capillary waves^{5,6}

$$\sigma_0^2 = \frac{k_B T}{2\pi\gamma} \ln\left(\frac{Q_{\text{max}}}{Q_{\text{min}}}\right) \quad (2)$$

where k_B is Boltzmann's constant, $Q_{\text{max}} = 2\pi/a$ ($a \approx 5 \text{ \AA}$ is on the order of intermolecular distance), and $Q_{\text{min}} = q_z^{\text{max}} \Delta\beta/2$. Equation 2 sets $\sigma_0 \approx 3.8 \text{ \AA}$.

I used Parratt formalism to extract from the data information about the electron density profile.¹¹ According to an X-ray reflectivity study of solutions with 50-, 70-, and 120- \AA particles, the structure of the *n*-hexane/silica sol interface can be described by models with nine or ten parameters, slicing the structure into three or four layers.⁴ For example, the solid line in Figure 2a represents a three-layer model with the profile and definition of the layers shown in Figure 3. Its model has nine independent parameters (Table 1). The dashed line in Figure 3 represents a four-layer model with ten parameters (see Table 2), similar to the resolution-based model discussed in ref 4. The contrast of the transition region is such that its structure factor has a Hilbert phase determined by the reflectivity only; the ambiguity of the electron density profile is associated with the limited q_z range covered in the reflectivity measurements.¹² Therefore, models with a large number of layers or/and parameters explain X-ray reflectivity with very similar profiles.

The wide interfacial structure between hexane and 70-\AA sol, $150\text{--}200 \text{ \AA}$, roughly consists of three parts, i.e., a thin $\sim 20\text{-\AA}$ layer with a high concentration of Na⁺ (compact layer), a monolayer of nanocolloidal particles as part of the thicker diffuse layer (Gouy layer), and a low-density $\sim 60\text{-\AA}$ layer of "surface water" sandwiched between them. These are the main elements

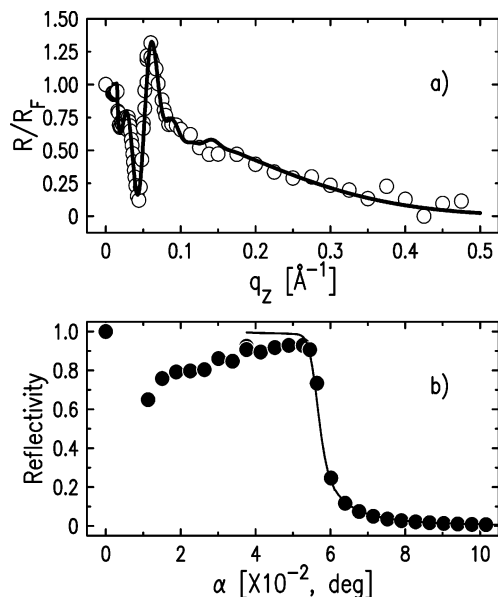


Figure 2. (a) X-ray reflectivity normalized to the Fresnel function at the *n*-hexane/silica sol interface (structure factor). The colloidal particles in the suspension are ~ 70 Å. The solid line represents the four-layer model. (b) X-ray reflectivity near the critical angle, $\alpha_c \approx (5.6 \pm 0.1) \times 10^{-2}$ deg ($q_c \approx 1.5 \times 10^{-2}$ Å $^{-1}$). The dots are the experimental data; the solid line is the four-layer model.

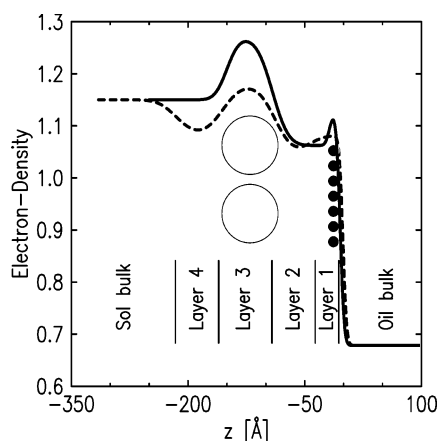


Figure 3. The normalized profiles to $\rho_w = 3.34 \times 10^{29}$ e $^{-}/\text{m}^3$ of the electron density across the *n*-hexane/silica sol interface of the three-layer (solid) and four-layer (dash) models with the definition of the layers. For clarity, the circles depict a monolayer of silica particles, and the dots represent the specifically adsorbed ions of Na $^{+}$ (Stern layer).

TABLE 1: Estimates of the Parameters in the Three-Layer Model^a (see Figure 3)

parameter	layer 1	layer 2	layer 3
l_i (Å)	20 ± 6	65 ± 8	60 ± 2
ρ_i	1.13 ± 0.01	1.06 ± 0.01	1.27 ± 0.02
σ_i (Å)	3.8 ± 0.1	16.5 ± 0.5	12 ± 1

^a l_i are the thicknesses of the interfacial layers with electron densities ρ_i , normalized to the density of water 3.34×10^{29} e $^{-}/\text{m}^3$ at normal conditions. $\sigma_0 = 3.8 \pm 0.1$ Å is the interfacial width of the boundary between the sol (layer 1) and hexane. The interfacial width between layer 1 and layer 2 $\sigma_1 = \sigma_0$. σ_2 is the interfacial width between the bulk of the electrolyte and the colloidal monolayer. σ_3 is the interfacial width between the low-density layer and the colloidal monolayer.

of the surface-normal structure that can be derived from the electron density profile.

In another experiment, I probed the density of the particles along the *z*-axis by a grazing incidence beam (see, for example, ref 13). With the incident angle, α , higher than the critical one, $\alpha_c \approx (5.6 \pm 0.1) \times 10^{-2}$ deg, the penetration length, Λ , for

TABLE 2: Estimates of the Parameters in the Four-Layer Model^a (see Figure 3)

parameter	layer 1	layer 2	layer 3	layer 4
l_i (Å)	42 ± 4	40 ± 4	68 ± 2	60 ± 2
ρ_i	1.10 ± 0.04	1.04 ± 0.01	1.19 ± 0.02	1.08 ± 0.02

^a l_i are the thicknesses of the interfacial layers with electron densities ρ_i , normalized to the density of water 3.34×10^{29} e $^{-}/\text{m}^3$ at normal conditions. $\sigma_0 = 3.8 \pm 0.1$ Å is the interfacial width of the boundary between the sol (layer 1) and hexane, and $\sigma = 18 \pm 2$ Å is the roughness for the other interfaces in the model.

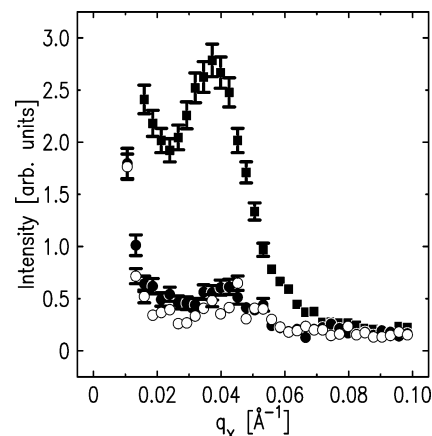


Figure 4. Small-angle scattering normalized to the reflected beam at $\phi = 0$ at the grazing incidence angles $\alpha \approx 0.04^\circ$ (squares, $\Lambda \approx 170$ Å), $\alpha \approx 0.035^\circ$ (dots, $\Lambda \approx 150$ Å), and $\alpha \approx 0.012^\circ$ (circles, $\Lambda \approx 140$ Å). The values of the reflected beam relative to the direct transmission beam ($\mathbf{q} = 0$) are shown in Figure 2b. The measurements of the grazing incidence small-angle scattering were conducted with spatial resolution of the detector $\Delta\beta = 0.2^\circ$ (along the *z*-axis) and $\Delta\phi = 4 \times 10^{-2}$ deg (along the *x*-axis).

X-rays is very large ($\Lambda \approx 10^5$ Å) so that most diffraction occurs in the bulk of the suspension. When α is smaller than the critical angle, the penetration length is

$$\Lambda \approx \Lambda_0 \left(1 + \frac{1}{2} \frac{\alpha^2}{\alpha_c^2} \right) \quad (3)$$

where $\Lambda_0 = \lambda/(2\pi \alpha_c) \approx 130$ Å. Thus, the grazing beam is mostly diffracted by the upper part of the interfacial structure. At $\alpha = 0.8\alpha_c$, the penetration length approximately equals the thickness of the transition layer ≈ 200 Å; at $\alpha = 0.3\alpha_c$, $\Lambda \approx \Lambda_0$.

Figure 4 shows “ q_x scans” taken at three incident angles $\alpha < 0.8 \alpha_c$. In this figure, the reflected beam is at $q_x = 0$. The intensity of the shoulder peak, $q_x \approx q_0$, which is associated with the principal ring of the small-angle scattering, decreases tenfold at small α . This decline represents a huge change, considering that the volume of the transition region, which contributes to diffraction, is reduced only by 30% (the same as the penetration length). On the other hand, the position of the maximum of the shoulder peak, which defines the particle–particle distance, is independent of α . This effect can be explained by the inhomogeneous interfacial structure with the electron density profile, shown in Figure 3, that contains the plane of the closest approach to the interface for the nanoparticles, above which the concentration of particles is at least ten times lower than in the bulk. The intensity of small-angle scattering depends strongly on α , since the plane is situated at the distance $\sim \Lambda_0$ from the oil’s surface.

Discussion

Earlier, Levine et al.¹⁴ studied the thermodynamics of emulsions stabilized by fine powders with van der Waals interactions

and capillary effects. Paunov et al.¹⁵ described a thermodynamic model of adsorption of slightly charged colloidal particles from an electrolyte solution. I note that in both papers the solid particles are assumed to congregate directly at the oil–water interface so that they are partially wet by both phases. These types of models cannot be applied to the hexane/sol interface, since silica nanoparticles have very hydrophilic surfaces with a large surface charge density of ~ 0.7 C/m².

Madsen et al.¹⁶ studied by X-ray scattering the interface of an air/silica solution of unspecified alkalinity containing particles significantly larger than ~ 300 Å in diameter. Their model for the surface-normal structure, based on data with very poor spatial resolution, $2\pi/q_z^{\text{max}} > 100$ Å, in the electron density profile, postulates three layers of silica particles near to the surface. However, the layered model cannot explain either our reflectivity data at high q_z or the angular dependence of the grazing incidence small-angle scattering at the *n*-hexane/silica sol interface.

In current classical electrochemistry, the electrical double layer is considered to be the inhomogeneous region of an electrolyte near a surface where the electrolyte ions are spatially separated. In the standard Gouy–Chapman–Stern model, the structure at the metal electrode/electrolyte solution interface consists of a compact layer (Stern layer) of adsorbed ions at the electrode's surface and a diffuse layer of ions (Gouy layer) with opposite charge that originates at a Helmholtz plane of closest approach to the electrode's surface and extends into the bulk of the solution.^{17–20} The effective thickness of the double layer is defined by a Debye screening length of the electrolyte solution. The surface-normal structure of the hexane/sol interface can be considered in the same manner as that of the electrode/electrolyte interface by analyzing the Poisson–Boltzmann equation under different conditions and system parameters.²¹ Volkov et al. offered a comprehensive insight into current status of the double layer theory at the oil/water interface.²²

The transition region at hexane/sol interface can be described in terms of a semiquantitative interface model discussed by Vorotyntsev and et al.²³ that suggests visualizing the surface of hexane and the Helmholtz plane for nanoparticles as two individual interfaces, contributing independently to the drop in potential across the interface. Although the surface-normal structure, which I discuss below, is a rough model neglecting a number of important factors that may be essential for describing the thick transition region at the hexane/sol interface, it is adequate for the quality of the available X-ray data (see ref 23).

Three factors may be involved in generating the potential gradient at the hexane/sol interface: a difference in the potentials of “image forces” between cationic Na⁺ and anions (nanoparticles); an adsorbed surface charge at the interface between the adsorbed layer and the solution; and a nonzero space charge in the adsorbed layer. First, the effect of “image forces” arises because of the different dielectric bulk properties of the phases in contact and because of the different planes of closest approach to the interface for the colloidal particles and Na⁺, which can be understood from the “classical” single-particle energy of interaction with the electrical image²⁴

$$\frac{Z^2}{16\pi\epsilon_0\epsilon_1} \frac{\epsilon_1 - \epsilon_2}{\epsilon_1 + \epsilon_2} \frac{1}{h} \quad (4)$$

where Z is a charge of the particle (ion), ϵ_0 is the dielectric permittivity of the vacuum, $\epsilon_1 = 78$ and $\epsilon_2 = 2$ are the dielectric permittivities of the water and hexane, respectively, and h is the distance from the center of the particle (ion) to the interface. Equation 4 explains quantitatively the main effect: the large Z

of the silica particle keeps it far from the interface to minimize energy. On the other hand, the plane of the closest approach for the sodium ions can reside very close to the oil boundary, so that the thickness of the compact layer (ion-free layer) is about the size of a water molecule.²⁵ I note that eq 4 does not correctly take into account the polarization of the interface and the changes of the dielectric properties of the media in the transition region. Second, the concentration of particles in layer 3, c_3^- , significantly exceeds that in the bulk concentration, c_b : $c_3^-/c_b \approx (\rho_3 - \rho_w)/(\rho_b - \rho_w) \approx 1.3–1.7$, where ρ_b and ρ_w are the electron densities of the sol bulk and water, respectively ($\rho_b \approx 1.15\rho_w$). Colloidal particles in this layer must carry a much higher charge than those in the bulk to stabilize the in-plane structure. This is accompanied by the additional adsorption of hydroxyl ions into this layer. Finally, the space charge in layer 1 and layer 2 is due to the spatial distribution of Na⁺. Sodium can infiltrate into the compact layer (Stern layer) because of its specific adsorption (reversible ionization of the hexane surface), caused by non-Coulombic short-range forces, and thereby form a compact or loose monolayer.²² There, the space charge density is low, and the relationships within the Gouy–Chapman theory can describe the potential distribution within layers 1 and 2 near the boundary with oil.²³

I note that a model in which there is no specific adsorption of sodium at the hexane surface cannot explain the profile of electron density. In that case, the space charge of layers 1 and 2 would be associated mainly with the ionic concentration of Na⁺. Therefore, the electric field would be zero at the oil boundary but at a maximum in layer 2 so that its electron density due to electrostriction would be greater than it is for layer 1, thereby contradicting the experiment. I suggest that the specific adsorption of Na⁺ is due to polarization of the hexane near the interface caused by the charge of the nanoparticles.

The surface concentration, Γ^+ , of specifically adsorbed Na⁺ can be estimated from the electron density profile by the following equation:⁴

$$\Gamma^+ \approx \left[0.1\Gamma - \frac{l_1}{V_0^w} \right] \left[1 + \frac{V^+}{V_0^w} \right] + \frac{l_1}{(V_0^w)^2} \delta V^w \quad (5)$$

where $V_0^w \approx 30$ Å³ is the volume per H₂O molecule in normal water, $V^+ \approx 4$ Å³ is the volume of Na⁺,²⁶ Γ is the integral number of electrons per unit area in the first layer ($\Gamma \approx l_1\rho_1$), and V^w is the volume per 10 electrons of the solvent (mixture of the solvent and silica) with an average electron density ρ_2 . According to Tables 1 and 2, V^w is less than V_0^w by $\approx 4–6\%$ ($dV/V = -d\rho/\rho$). Equation 5 is valid when both $\delta V^w/V_0^w = |V^w - V_0^w|/V_0^w \ll 1$ and $V^+/V_0^w \ll 1$. The surface charge density of Na⁺ in the Stern layer, $e\Gamma^+$, ranges between 0.6 ± 0.3 C/m² and 1.5 ± 0.5 C/m² for the three-layer (see ref 4) and four-layer models, respectively, so that these models set the high and low limits for $e\Gamma^+$.

A simple estimation using the bulk properties of the sol shows that a layer as wide as $L = \Gamma^+/(c^+N_A)$ near the interface must be poor in sodium to create the compact layer. $L \approx 300$ Å for the three-layer model, and it is two or three times wider for the four-layer model. Therefore, specific adsorption depletes the entire transition layer of sodium ions, so considerably increasing the Debye screening length in layer 2. The electric field, E , which in the first approximation can be considered as a constant $E = \Gamma^+/\epsilon_0 \approx 10^9–10^{10}$ V/m (ϵ is the dielectric permittivity of water in the layer, $\epsilon < \epsilon_1$), may significantly change the water density in layer 1 and 2 due to electrostriction.³

In the first approximation, the colloidal silica is a mixture of water and amorphous silica. The following equation defines the

bulk electron density of the sol with a volume content of nanoparticles, f_b :

$$\rho_b = f_b \rho_{\text{SiO}_2} + (1 - f_b) \rho \quad (4)$$

where ρ_{SiO_2} and ρ are the average bulk electron densities of silica particles and water, respectively. I note that the value of ρ within the accuracy of the experiment is equal to the density of water under normal conditions, $\rho_w = 3.34 \times 10^{29} \text{ e}^-/\text{m}^3$.²⁷

The following equation, similar to eq 4, relates the volume content of silica in the low-density layer, $f_2 \ll 1$, with its electron density ρ_2 :

$$\rho_b = f_2 \rho_{\text{SiO}_2} + (1 - f_2) \rho' \quad (5)$$

where $\rho' = \rho + \delta\rho$ describes the difference between the average density of water in the bulk and the "surface water", $\delta\rho/\rho \ll 1$. Then, by excluding ρ_{SiO_2} from the composition eqs 4 and 5 and omitting the term $\propto f_2 \delta\rho$, the following expression is obtained:

$$\frac{\delta\rho}{\rho} \approx \frac{\rho_2}{\rho} - 1 - \frac{f_2}{f_b} \left(\frac{\rho_b}{\rho} - 1 \right) \quad (6)$$

The electron density of the intermediate low-density layer 2 sets the high limit for the density of "surface water", since it separates the positive and negative charge in layer 1 and layer 3, respectively. The low limit follows from the small-angle scattering data. For uniform particles, the ratio is $f_2/f_b \approx c_2^-/c_b^-$ (see ref 28), where, according to the small-angle scattering data, $c_2^-/c_b^- < 0.1$. The variation of the electron density in the region between layer 1 and the monolayer of nanoparticles (parameter ρ_2/ρ in eq 6) falls for different models between 1.04 and 1.07, so that $0.01 < \delta\rho/\rho < 0.07$. The result is not affected by taking into account a small concentration of Na^+ in layer 2 (or even as much as in the bulk). Thus, the average water density in the field of $\sim 10^9$ – 10^{10} V/m of the electric double layer at the hexane/silica sol interface is only few percent higher (1–7%) than the water density under normal conditions. I note that the layer of "surface water" is so thick the capillary waves at the hexane/sol interface could not hide the effects of its density. In fact, this estimation of $\delta\rho/\rho$ is considerably lower than the values calculated earlier for the density of water in the first layer of molecules at the electrode's surface with a similar surface charge.³

A comparison with the calculations of I. Danielewicz-Ferchmin and A. R. Ferchmin would not be valid if the charge in the compact layer were screened by a diffuse layer of OH^- located near the surface with hexane. However, this situation is unlikely: there is a huge deficit of free hydroxyl ions in the solution that would prevent the buildup of any significant countercharge in layer 1. Unfortunately, to test such a model that describes, for example, a variation of electrolyte concentration in the "surface water" layer, the spatial resolution of the X-ray scattering experiment must be improved significantly.

Acknowledgment. Brookhaven National Laboratory is supported by U.S.D.O.E., contract no. DE-AC02-98CH10886. X19C is partially supported through funding from the Chem-MatCARS National Synchrotron Resource and the University of Chicago. I thank Professor Mark L. Schlossman for valuable discussions. I also thank Avril Woodhead.

References and Notes

(1) Toney, M. F.; Howard, J. N.; Richer, J.; Borges, G. L.; Gordon, J. G.; Melroy, O. R.; Wiesler, D. G.; Yee, D.; Sorensen, L. B. *Nature (London)* **1994**, *368*, 444.

(2) Wang, J.; Ocko, B. M.; Davenport, A. J.; Isaacs, H. S. *Phys. Rev. B* **1992**, *46*, 10321.

(3) Danielewicz-Ferchmin, I.; Ferchmin, A. R. *J. Phys. Chem.* **1996**, *100*, 17281.

(4) Tikhonov, A. M. *J. Chem. Phys.* Submitted.

(5) Buff, F. P.; Lovett, R. A.; Stillinger, F. H. *Phys. Rev. Lett.* **1965**, *15*, 621.

(6) Mitrinovic, D. M.; Zhang, Z.; Williams, S. M.; Huang, Z.; Schlossman, M. L. *J. Phys. Chem. B* **1999**, *103*, 1779. Mitrinovic, D. M.; Tikhonov, A. M.; Li, M.; Huang, Z.; Schlossman, M. L. *Phys. Rev. Lett.* **2000**, *85*, 582.

(7) In the first Born approximation, the contribution of the transition region at the *n*-hexane/water interface into the structure factor is $(\rho_m - \rho_w)/(\rho_w - \rho_{\text{oil}}) > 20$ times stronger than it is at a metal/electrolyte interface, where ρ_m is the electron density of metal, $\rho_w = 3.34 \times 10^{29} \text{ e}^-/\text{m}^3$ is the electron density of water, and $\rho_{\text{oil}} = 2.28 \times 10^{29} \text{ e}^-/\text{m}^3$ is the electron density of *n*-hexane (see ref 4). The electron densities of Ag and Au are $\rho_{\text{Au}} = 4.66 \times 10^{30} \text{ e}^-/\text{m}^3$ and $\rho_{\text{Ag}} = 2.76 \times 10^{30} \text{ e}^-/\text{m}^3$, respectively.

(8) The total thickness of the surface-normal structure of the transition layer at the electrode/electrolyte solution of simple inorganic ionic salts, such as those studied by Toney et al.¹ and Wang et al.,² was roughly 10–20 Å wide, which is defined by the Debye length in the electrolyte solution. These structures were resolved by reflectivity data with a relatively fine spatial resolution in the electron density profile (~ 1 Å), which would require reflectivity measurements at the hexane/sol interface at levels below 10^{-12} . Since bulk scattering of 15 keV X-ray beam in *n*-hexane limits reflectivity measurements to as low as 10^{-9} , the typical spatial resolution in the experiment at the hexane/water interface at X19C is ~ 10 Å.

(9) Schlossman, M. L.; Synal, D.; Guan, Y.; Meron, M.; Shear-McCarthy, G.; Huang, Z.; Acero, A.; Williams, S. M.; Rice, S. A.; Viccaro, P. J. *Rev. Sci. Instrum.* **1997**, *68*, 4372.

(10) Guinier, A. *X-ray Diffraction In Crystals, Imperfect Crystals and Amorphous Bodies*; Dover Publications: New York, 1994.

(11) Parratt, L. G. *Phys. Rev.* **1954**, *95*, 359.

(12) Clinton, W. L. *Phys. Rev. B* **1993**, *48*, 1.

(13) Tolan, M. *X-ray Scattering from Soft-Matter Thin Films*; Springer Tracts in Modern Physics 148; Springer: New York, 1999.

(14) Levine, S.; Sanford, E. *Can. J. Chem. Eng.* **1985**, *62*, 258. Levine, S.; Bowen, B. D.; Partridge, S. *Colloids Surf.* **1989**, *38*, 325. Levine, S.; Bowen, B. D.; Partridge, S. *Colloids Surf.* **1989**, *38*, 345.

(15) Paunov, V. N.; Binks, B. P.; Ashby, N. P. *Langmuir* **2002**, *18*, 6946.

(16) Madsen, A.; Konovalov, O.; Robert, A.; Grubel, G. *Phys. Rev. E* **2001**, *64*, 61406.

(17) Gouy, G. *J. Phys.* **1910**, *9*, 457.

(18) Chapman, D. L. *Philos. Mag.* **1913**, *25*, 475.

(19) Stern, O. *Z. Elektrochem.* **1924**, *30*, 508.

(20) Adamson, A. W. *Physical Chemistry of Surfaces*, 3rd ed.; John Wiley & Sons: New York, 1976.

(21) Verwey, E. J. W.; Nielsen, K. F. *Philos. Mag.* **1935**, *28*, 435.

(22) Volkov, A. G.; Dreamer, D. W.; Tanelli, D. L.; Markin, V. S. *Liquid Interfaces in Chemistry and Biology*; John Wiley & Sons: New York, 1998. Volkov, A. G.; Dreamer, D. W.; Tanelli, D. L.; Markin, V. S. *Prog. Surf. Sci.* **1996**, *53*, 1.

(23) Vorotyntsev, M. A.; Ermakov, Yu. A.; Markin, V. S.; Rubashkin, A. A. *Russ. J. Electrochem.* **1993**, *29*, 730.

(24) Landau, L. D.; Lifshitz, E. M. *Electrostatics of Dielectrics. In Electrodynamics of Continuous Media*, 2nd ed.; Pergamon: New York, 1984; Chapter 2.

(25) Girault, H. H. J.; Schiffrin, D. J. *J. Electroanal. Chem.* **1983**, *150*, 41.

(26) Huheey, J. E.; Keiter, E. A.; Keiter, R. L. *Inorganic Chemistry: Principles of Structure and Reactivity*, 4th ed.; Harper Collins: New York, 1993.

(27) Both $f_b \rho_{\text{SiO}_2} = (1.08 \pm 0.01) \times 10^{29} \text{ e}^-/\text{m}^3$ and $(1 - f_b) \rho = (2.73 \pm 0.01) \times 10^{29} \text{ e}^-/\text{m}^3$ can be determined with very high accuracy from the weight of the silica dried and annealed at high temperature, ν , per unit volume of sol ($\nu = 30.5\%$) so that $\rho_b = (3.81 \pm 0.02) \times 10^{29} \text{ e}^-/\text{m}^3$. On the other hand, $\rho_b = (3.9 \pm 0.1) \times 10^{29} \text{ e}^-/\text{m}^3$ can be estimated from the value of the critical angle for the hexane/silica sol interface, $\alpha_c = \lambda \sqrt{r_e(\rho_b - \rho_h)/\pi} \approx (5.6 \pm 0.1) \times 10^{-2} \text{ deg}$, where $r_e = 2.814 \times 10^{-5} \text{ Å}$ is the Thompson scattering length of the electron and $\rho_h = 2.30 \times 10^{29} \text{ e}^-/\text{m}^3$ is the electron density of *n*-hexane. Therefore, eq 4 describes the silica sol bulk very accurately, and $\rho = (1 - \nu) \rho_b$ is as much as $(3.3 \pm 0.1) \times 10^{29} \text{ e}^-/\text{m}^3$.

(28) If the nanoparticles in the suspension are uniform, then the volume content of the silica $f = c\nu$, where $\nu \approx (\pi/6)D^3$ is the average volume per particle and c is the volume concentration of the particles.